Science of the Total Environment 810 (2022) 152258

Contents lists available at ScienceDirect

Science of the Total Environment

journal homepage: www.elsevier.com/locate/scitotenv

Recovery of rare earth elements from acidic mine waters: An unknown secondary resource

M. Hermassi [a], M. Granados [b], C. Valderrama [c], C. Ayora [d], J.L. Cortina [c,e,*]

[a] Thermochemical Energy Conversion Laboratory, Department of Applied Physics and Electronics, Umeå University, SE-90187 Umeå, Sweden
[b] Analytical Chemistry and Chemical Engineering Department, University of Barcelona, V. Diagonal 647, 08028 Barcelona, Spain
[c] Chemical Engineering Department, East Barcelona Engineering School, Barcelona TECHUPC, Eduard Maristany 10-14 (Campus Diagonal-Besòs), 08930 Sant Adrià de Besòs, Spain
[d] Institute of Environmental Assessment and Water Research (IDAEA-CSIC), Jordi Girona 18, 08034 Barcelona, Spain
[e] Water Technology Center CETaqua, Carretera d'Esplugues 75, 08940 Cornellà de Llobregat, Spain

HIGHLIGHTS

- Rare earth recovery from acid mine drainage
- Effective process to treat acid mine drainage to concentrate and recover rare earth elements
- Integration of selective phosphate precipitation with ion-exchange concentration
- Selective separation of rare earth elements from transition elements

GRAPHICAL ABSTRACT

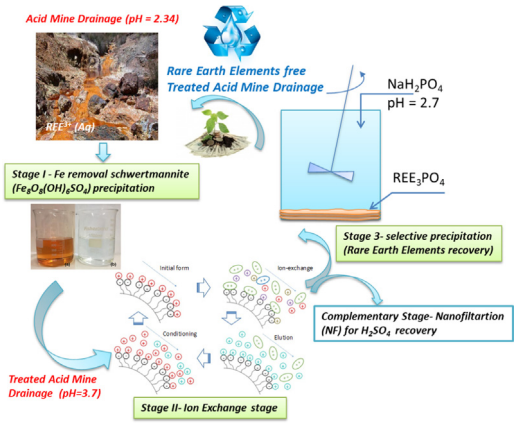

ARTICLE INFO

Article history:
Received 30 October 2021
Received in revised form 2 December 2021
Accepted 4 December 2021
Available online 10 December 2021

Editor: Damià Barceló

Keywords:
Acid mine drainage
Sulfonic resin
REE recovery
Ionic exchange
Separation
Phosphate precipitation

ABSTRACT

Acidic mine Drainage (AMD) is still considered one of the greatest mining sustainability challenges due to the large volumes of wastes generated and the high associated treatment cost. New regulation initiatives on sustainable development, circular economy and the need for strategic elements as Rare Earth Elements (REE) may overcome the traditional research initiatives directed to developing low cost treatment options and to develop research initiatives to identify the potential benefit of considering such AMD as a potential secondary resource. As an example, this study develops the integration of a three-stage process where REE are selectively separated from base metals (e.g. Fe, Al, Mn, Ca, Mg, Cd, Pb) and then concentrate to produce a rich REE by-product recovered as REE-phosphates. Selective separation of Fe (>99%) was achieved by total oxidation to Fe(III) and subsequent precipitation as schwertmannite at pH 3,6 ± 0.2. REE were then extracted from AMD using a sulfonic ion-exchange resin to produce concentrated REE sulfuric solutions up to 0.25 gREE/L. In a final stage selective separation of REE from Al(III), Ca(II) and Mg(II) and transitions elements (Cu, Zn, Ni) was achieved by precipitation with phosphate solutions under optimized pH control and total phosphate concentration. XRD analysis identified low-crystalline minerals. By using a thermal treatment the presence of $PrPO_4$(s) and Cheralite ($CePO_4$(s)) where Ce is substituted by La and Ca and Xenotime (YPO_4(s)) were found as main minerals $AlPO_4$(s) Ca,$MgYPO_4$(s) were also identified.

* Corresponding author at: Chemical Engineering Department, East Barcelona Engineering School, Barcelona TECHUPC, Eduard Maristany 10-14 (Campus Diagonal-Besòs), 08930 Sant Adrià de Besòs, Spain.
E-mail address: jose.luis.cortina@upc.edu (J.L. Cortina).

http://dx.doi.org/10.1016/j.scitotenv.2021.152258

1. Introduction

Mining activity in the Iberian Pyrite Belt (South of the Iberian Peninsula) has led to the presence of many sources of acid mine drainage (AMD) as it is the case of the Tinto and Odiel rivers. AMD are characterized by a low pH (2–4) and high concentration metallic species (e.g., Fe, Al, Cu) and non-metallic species (e.g., As, Se, Sb) (Akcil and Koldas, 2006). The generation of AMDis the oxidation of sulfide minerals disposed tailings and waste dumps, which are not stable when exposed to water and oxygen (Ayora et al., 2016; Ayora et al., 2015; López et al., 2019a; Simate and Ndlovu, 2014). Among the metallic species, rare earth elements (REE) are typically resent in concentrations up to 1000 times higher than those in natural water bodies (Ayora et al., 2016; López et al., 2019a; Olías et al., 2018).

The most common means to treat AMD is via neutralization with alkaline reagents such as lime, limestone, sodium carbonate or ammonia which generates large volumes of sludge (Evangelou and Zhang, 1995). This sludge is essentially made up of Fe and Al hydroxysulfates, and due to its high water content, disposal and storage of this waste represents a major operating cost and environmental concern for coal and base metal mining operations (Ackman, 1982; Viadero et al., 2006). On the other hand, passive remediation systems neutralize AMD by intercepting its natural flux with a permeable filter of limestone (Hedin et al., 1994; Ayora et al., 2013). Along this process, a sequential precipitation of Fe and Al phases occurs obtaining two well-differentiated layers of these solids. The Fe will initially precipitate at pH 3 to 5 depending on its oxidation state. The Al phase is then precipitated at pH values from 4.5 to 6 which is where most of REE is also precipitates out.

Given REE are considered critical industrial raw materials, with relevant applications in electronics, superconductor, permanent magnet, medical, and nuclear technologies (Kulczycka et al., 2016; Zhang et al., 2017). Therefore, their recovery from secondary resources as mining tailings and AMD is a challenging opportunity (Hermassi et al., 2021; Samonov, 2011; Nleya et al., 2016). This serves as a motivation for the development of new techniques, both economical and sustainable, aimed at their recovery and solves this unwanted consequence or damage to the environment (Binnemans et al., 2013; Machacek et al., 2015). The main source of lighter REE (La, Ce, Pr, Nd) and heavier REE (Ho, Er, Tm, Yb, Lu, Y) in nature are monazite ((REE,Th)PO_4) and bastnesite (REE(CO_3)F) minerals (Gupta, 2005; Habashi, 2013). Production of REE from such minerals require complex mineral processing and purification stages and a reliable way to develop a sustainable and economical valorisation route could be to recover REE present in AMD as rich REE mixture of phosphates (REE-phosphates) minimizing the presence of transition metals (Al and Fe).

A second challenge to be solved is the fact that they are present at low concentration levels (μg to mg/L) and the development of a novel process economical viable should be focused on the selective recovery of such valuable elements at low concentration values. The most established technologies including solvent extraction, precipitation and ion exchange have been applied to concentrate streams (Jorjani and Shahbazi, 2016; Riley and Dutrizac, 2017; Iftekhar et al., 2017; Vaziri Hassas et al., 2020). Hence, the development of novel processes focusing on the selective recovery of REEs at low concentrations is a present challenge Selective removal of Fe after oxidation to Fe(III) by precipitation at pH above 3.7, and subsequent recovery of valuable metals (including Cu, Zn, and REEs) by sorption and ion-exchange (IX) processes has been identified as an innovative option for a more sustainable AMD management compared to the traditional treatments (Khawassek et al., 2015; Wu et al., 2018; Ramasamy et al., 2019). However, reduced metal concentration factors reached in the sorption stages due to the presence of other metallic species (López et al., 2019a). The integration of pressure driven membrane technologies to manage metal containing acidic streams as nanofiltration (NF) (López et al., 2019a; Mullett et al., 2014; Zhong et al., 2007), forward osmosis (Pramanik et al., 2019) or electrodialysis (ED) (Al-Zoubi et al., 2010; Martí-Calatayud et al., 2014) could solve these problems. NF shows high rejections of multi-charged ionic species, while the transport of single-charged ionic species (e.g., H^+, HSO_4^-) is favoured (López et al., 2019a), but the concentration factors achieved as single treatment stage are not efficient enough to develop economical and sustainable recovery processes (Meschke et al., 2018; López et al., 2018a). Recently, Lopez et al., (López et al., 2018b; López et al., 2019b) demonstrated that the use Desal DL NF membrane provided metal concentration factors around 1.5 and the REE concentrations with up-to 0.2 g REE/L are a suitable source to precipitate mixtures of REE-phosphates ($REEPO_4$(s)) by using phosphate salts at pH values around pH 2.5 to 2.7. At these pH values, the precipitation of Al, Zn and Cu, would be minimized and the by-product generated would be mineral that could be used as raw-material in the production of REEs (López et al., 2019a; Wang et al., 2017).

The main objective of this work was to evaluate the performance of the integration of: i) a preliminary stage of removal of Fe from AMD containing REE using CaO(s), MgO(s) or NaOH; ii) a second stage where the Fe-free treated AMD (TAMD) containing REE is concentrated by using a IX resin containing a sulfonic group and ii) a selective precipitation stage using phosphate salts at fix pH is used to recover REE as phosphates. In addition to CaO(s), the most commonly used alkaline reagent used for neutralization of acidic waters, as it is providing Ca(II) as by-product that will potentially consume phosphate, two other alkaline solutions MgO(s) and NaOH with lower tendency to consume phosphate were also investigated. The selective precipitation of REE-phosphates with the minimum presence of transition metals was evaluated by using batch experiments. One of the main interferences could be the presence of Al(III), which is not removed in first stage of Fe removal, and their presence on the mixed REE-phosphates was evaluated.

2. Selective recovery of REE by phosphate precipitation: fundamentals

The aqueous chemistry of the system REE(PO_4)–(SO_4)–H_2O (25 °C) were made with the code PHREEQC 3.3 (Parkhurst and Appelo, 1999) and the Donnee Thermoddem_V1.10.dat database compiled by Bureau de Recherches Géologiques et Minières, BRGM (Blanc et al., 2012). The thermodynamic data for schwertmannite and basaluminite are those referred to by Sánchez-España et al. (2011). Data showed that REE-hydroxides (REE(OH)$_3$) precipitate in alkaline solutions (i.e. pH > 7.5), while $REEPO_4$ are formed at acidic conditions. The thermodynamic calculations were used to perform an initial definition of the experimental conditions in terms of pH and phosphate concentration that could be used to develop a REE recovery from AMD. As it is shown in Fig. 1, solubility of metal hydroxides of Fe(III), Al(III), the low solubility of Fe(III) species in solution above pH 3.7, implies the need to remove selectivity iron and sulfate ions, major components of AMD, by precipitation of schwertmannite as has demonstrated experimentally by Ayora et al. (2016).

At pH values below 3.7, Al(III) not precipitate as basaluminite ($AlOHSO_4$(s)). The formation of Al(III) and divalent transition elements (TE) hydroxides occur at pH higher than 6, and needs to be avoided to prevent REE losses to the precipitate. The formation of REE-PO_4, assuming typical values of 10^{-5} mol/L in AMD, initiates at pH above 2.0 and finalizes (>99% precipitated and log[M] = −8) at pH values below 3.1. As shown in Fig. 2, the precipitation of REE-PO_4 started above pH 2.2 and could be considered complete (>99%) above pH 3.2, with the exception of Y, with a slightly different behaviour as its precipitation stars at pH above 2.5.

For all the elements considered, the more stable mineral phase was the corresponding REE-PO_4, TE-PO_4, with the exception of Fe(III) and Al(III) which the more stable mineral phase was schwertmannite and basaluminite, respectively.

Precipitation of divalent transition metals as Zn (TE-PO_4) occurs at higher pH values while other elements present at low levels are not precipitating (Cd, Co) but could slightly precipitate with (Cu) (Fig. 1). Only Al (III)-PO_4 started precipitation above pH 3.7. Then, in this study the experimental effort was focused on the optimization of the reduce pH window where most of the REE have been precipitated as phosphates with the minimum presence of $AlPO_4{\cdot}2H_2O$(s).

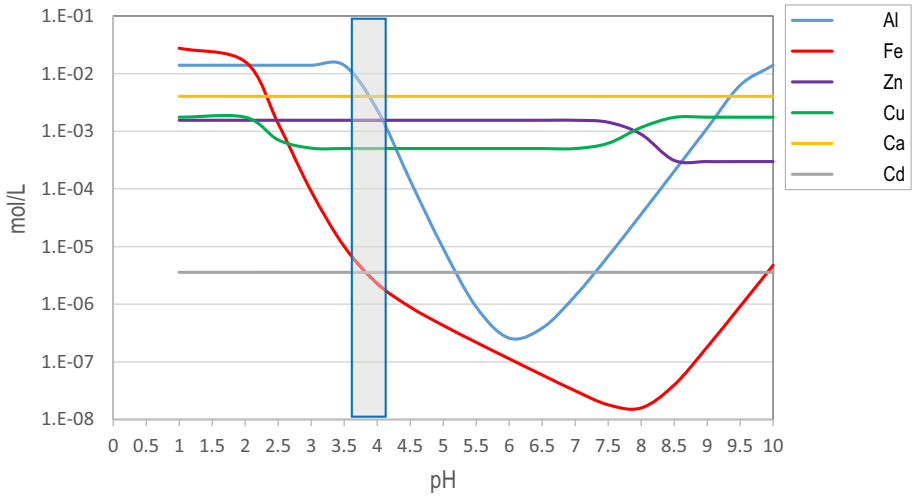

Fig. 1. Variation of the solubility with pH of schwertmannite (FeIII), basaluminite (Al), hopeite(α) (Zn), $Cu_3(PO_4)_2$ (Cu) and $Co_3(PO_4)_2$ (Co). The shaded rectangular field is the pH to achieve a quantitative removal (95–99%) of Fe and to minimize the precipitation of Al (<3%).

3. Experimental methodology

3.1. Iron removal experiments

REE standard solutions: La(III), Y(III), and Ce(*III*)solutions of 1.g REE/L were prepared using $La_2(SO_4)_2c(s)$, $Y_2O_3(s)$ and $CeCl_3$ (s) after appropriate dissolution with deionized water (1% (w/w) H_2SO_4). Nd(III), Dy(III) and Yb(III) standard solutions of 1.g/L in HNO_3 1% were used to make the synthetic solutions.

Batch experiments with AMD collected from La Poderosa Mine (Huelva, Spain), were carried out following several stages. In a first stage Fe(II) was quantitatively oxidized by H_2O_2 (>99,9%) and then Fe(III) present in solution was removed by addition of three different alkaline reagents (CaO(s), MgO(s) and NaOH) at a room temperature. Hydrogen peroxide has been used for practical experimental simplicity to achieve a successful oxidation of Fe(II) to Fe(III). Although it is more widely used oxidation by air bubbling it should be mentioned that engineering companies in the mining sector are commercializing oxidation stages with H_2O_2. Their use is recommended as it is this case where the content of Fe(II) is not high.

Precipitation tests carried out were in three separate batch 1 L AMD which had been pre-oxidized by H_2O_2, before adding the appropriate amount of either NaOH solution (50%), CaO(s) (99%) or MgO(s) (99.5%) to each test, respectively, until the pH reach a value of 3.6 ± 0.2. This value, according to previous studies, ensure a quantitative removal of Fe (III) (>99%) from solution and minimum removal (<2%) of TR, REE and Al(III). Due to their low solubility of CaO (s) and MgO (s) in aqueous solutions testing solutions (CaO, MgO slurries) were prepared by using ultrasounds.

On completion of target neutralization pH, the solution was filtered by using columns of 15 cm diameter and 30 cm length containing quartz sand (100–200 μm). Filtration was performed under gravity (down flow). Filtered water samples of each alkaline treatment were used in further stages. Composition of the samples was determined by using ion chromatography, ICP-OES as well as ICP-MS. Solutions pH were measured by using a combined pH electrode (Crison) (Hermassi et al., 2021).

3.2. REE concentration experiments by ion exchange

Purolite SPC11706 (Purolite, Spain), a macro-porous IX resin with a cross-linked DCB-PS matrix cation exchange resin containing sulfonic groups, macroporous IX resin with a cross-linked DVB-PS matrix. Resin was provided in sodium form and was conditioned before used as described elsewhere (Reig et al., 2019). Analytical grade reagents, such as CaO(s), MgO(s), NaOH, HCl, and H_2SO_4, were used to adjust pH of working solutions and to prepare the regeneration solutions. All solutions were prepared using Milli-Q (Merck-Millipore) water quality (Hermassi et al., 2021).

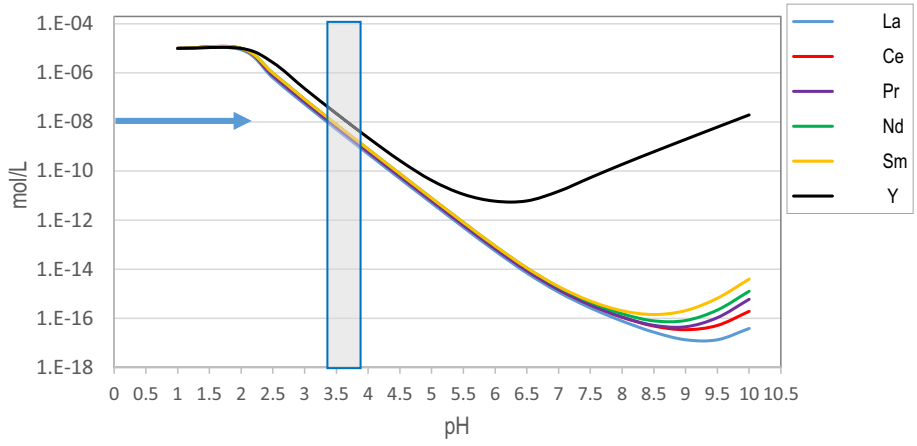

Fig. 2. Variation of the solubility of the REE-PO_4phases with pH Phosphate and Total REE concentrations were fixed at 10^{-3} and 10^{-5} mol/L, respectively. The concentration of Al, Fe, Zn, Cu and Co were those of the Poderosa acid mine drainage (Table 1). The vertical rectangular fields indicate the pH values to be set-up after the phosphate addition.

An Omnifit glass column 10 cm long and 1.5 cm of internal diameter, filled with 9.5 ± 0.5 g of resin was used. To pump the different Fe-free treated AMD (TAMD) solutions through the column a peristaltic pump (Minipuls 3, Gilson MP) was used. A fraction collector (FC 204 Gilson) was arranged at the exit of the column. Before starting each experiment, the column was equilibrated with deionized water. Then, TAMD was acidified to pH 2.1 to increase the selectivity factor for REE recovery and pumped at 1 mL/min through the column and samples were collected by the fraction collector. Finally, the elution stage was performed by using 1 M H_2SO_4 at a 0.25 mL/min flow rate. The samples collected, in the sorption an desorption stages,were filtered at 0.22 μm (SimplePIure 13 mm), acidified with pure HNO_3 to reach 1%(w/w) concentration and stored at 4 °C until analysis. The breakthrough curves and elution curves were calculated as a function of the treated bed volumes of TAW or elution solution, respectively. The treated volume was expressed as Bed Volume (BV) defined by Eq. (1):

$$BV = \frac{V_s}{V_b} \quad (1)$$

where V_S is the treated volume and V_b is the column pores volume determined from a tracer assay as described elsewhere (Reig et al., 2019).

3.3. Selective recovery of REE by phosphate precipitation at fixed pH

REE recovery from TAMD was investigated in batch experiments. The objective was to identify the optimal conditions (pH and phosphate stoichiometric excess) to obtain the maximum recovery of REE by precipitation of $REE(PO_4)_{(s)}$ and to minimize the precipitation of transition elements ($TEPO_4(s)$). The different experimental conditions evaluated were: a) precipitation experiments as a function of pH; b) precipitation as a function of the acid nature to fix pH using mixtures of NaH_2PO_4 with HCl, H_3PO_4 and H_2SO_4; and c) precipitation experiments as a function of the phosphate molar stoichiometric excess (SQ) defined by equation Eq. (2):

$$SQ = \frac{\sum H_X PO_4^{x-3} added\ (mol)}{\sum REEt\ (mol)} \quad (2)$$

where $\Sigma H_xPO_4^{x-3}$ represents the total number of moles added as NaH_2PO_4 or H_3PO_4, and ΣREE_t represents the total number of moles of REE present on the acid water to be treated.

Appropriate amounts of NaH_2PO_4 for a given SQ value and acid (HCl, H_2SO_4, H_3PO_4) was added to 20 mL of TAMD in glass tubes at room temperature. Samples were equilibrated for 24 h in an overhead shaker to assure to reach equilibrium at fixed pH and maintained in agitation for 24 h more. At the end of the experiments, samples were filtered at 0.22 μm, acidified with pure HNO_3 and stored at 4 °C until analysis.

The optimum pH conditions to achieve quantitative precipitation of REE was carried out using synthetic solutions of Ce(III) and La(III) as model elements and phosphate dosing was evaluated by using mixtures of NaH_2PO_4. Different strong acids (e.g., H_2SO_4, HCl and H_3PO_4) were used to study the influence of the complexing properties of other anions as chloride.

3.4. Aqueous samples analytical techniques

Measurement of pH was made using a Crison® glass electrode calibrated with buffer solutions of pH 7 and 4. Major cations (Ca, Mg, Zn, Fe, Mn, Si) and total S were measured by ICP-AES (Perkin-Elmer® Optima 3200 RL) and trace metals (Ni, Cd, Co, Pb, REE) with ICP-MS (Perkin-Elmer®Sciex Elan 6000). Detection limits were 0.1 mg/L for S; 0.05 mg/L for Ca, Mg, Si; 0.02 mg/L for Fe, Zn, Mn; 5 μg/L for Al; 1.5 μg/L for Cu, Ni; 0.5 μg/L for Pb; 0.2 μg/L for Cd, Co and REE (Hermassi et al., 2021). The analytical precision error was estimated to be approximately 5% for ICP-AES and 4% for ICP-MS measurements. Assuming all S to be sulfate, the charge balance error was usually less than 5% for the Poderosa mine water and less than 10% for the synthetic solution.

3.5. Solid samples analytical techniques

Precipitates were analysed by powder X-ray diffraction (XRD) to determine the composition and the major mineral phases of the crystalline content in the samples. The samples were homogenized and, if necessary, ground, before analysis. Analyses were made on a Bruker® D5005 X-Ray Diffractometer in θ–θ mode with Cu Kα radiation. Repeated continuous scans were performed on rotating samples in the 2θ range 0–60° at a rate of 0.025°/18 s.

Precipitates were also observed under a JEOL® JSM840 Field Emission Scanning Electron Microscope with Oxford Link® Energy Dispersive System (SEM-EDS).

4. Results and discussion

4.1. Characterization of the Poderosa AMD and removal of Fe(II)/Fe(III) from AMD

The REE concentrations in the Poderosa acid mine water are summarized in Table 1. The concentration of REE ranged from 0.01 mg/L for Lu up to 3.3 mg/L for Ce at pH of 2. Two main groups could be defined with most of the Heavier REE (HREE) (Tb, Dy, Ho Er, Tm, Yb, Lu and Y) and Eu in the range 0.01 to 1.79 mg/L and Lighter REE (LREE) (La, Ce, Pr, Nd, Sm, Eu and Gd) in the range 0.4 to 3.3 mg/L. For the case of transition elements (TE) the highest concentrations was Fe, at 1.5 g Fe/L, followed by a group of elements between 0.1 and 0.4 g/L (Al, Mg, Ca, Cu and Zn) and a group of elements below 10 mg/L (Co, Ni, Cd, Hf, Y).

Fig. 3 shows the removal (%) of both TE, REE and Fe(III) after the oxidation of Fe(II) to Fe(III) and the alkaline treatment of the AMD by CaO (s), MgO(s) and NaOH (values before and after the treatment are reported in (Table 2)). As shown in Fig. 3 the AMD treated with CaO(s) had the highest removal (around 8% at pH < 3.8–3.9) of the targeted REEs.

The pre-treatment with NaOH provided the lowest removal ratios of REEs being the preferred and recommended from the point of view of not increasing the concentration of Mg(II) and Ca(II), and not a potential consumer of phosphate ions, but its use will need to be evaluated economically due to its higher cost. In relation to Fe elimination the three pre-treatments provided similar removal ratios (>99.9%). However, in terms of aluminium removal the pre-treatment with CaO (s) exhibited the lowest percentage of removal. XRD analysis of the sludge generated, was a brown to orange colour, which was identified as schwertmannite [$Fe_8O_8(OH)_6SO_4{\cdot}nH_2O$].

As no REE were partially lost in schwertmannite precipitates, the REE content was proposed to be entirely recovered from AMD treated with alkaline reagents to pH 3.7 (TAMD). If pH increased above 4.7, Al(III) would

Table 1
REEs, as Light Rare Earth Elements (LRRE) and Heavy Rare Earth Elements (HREE) and transition metals (TE) concentrations in the acid mine water sample (mg/L) from the Poderosa mine.

	REE	mg/L	TE	mg/L
LREE	Eu	0.07 ± 0.01	Fe	1535 ± 28
	Pr	0.44 ± 0.04	Al	375 ± 20
	Sm	0.51 ± 0.04	Ca	161 ± 23
	Gd	0.54 ± 0.07	Mg	182 ± 25
	La	1.21 ± 0.2	Cu	111 ± 15
	Nd	1.94 ± 0.3	Zn	101 ± 15
	Ce	3.28 ± 0.4	Co	1.4 ± 0.2
HREE	Lu	0.01 ± 0.002	Cd	0.4 ± 0.05
	Tm	0.02 ± 0.002	Ni	0.3 ± 0.04
	Ho	0.02 ± 0.002	Hf	0.37 ± 0.04
	Dy	0.40 ± 0.04	Y	1.79 ± 0.2
	Tb	0.09 ± 0.01	–	——
	Yb	0.10 ± 0.02	—	
	Er	0.15 ± 0.02		

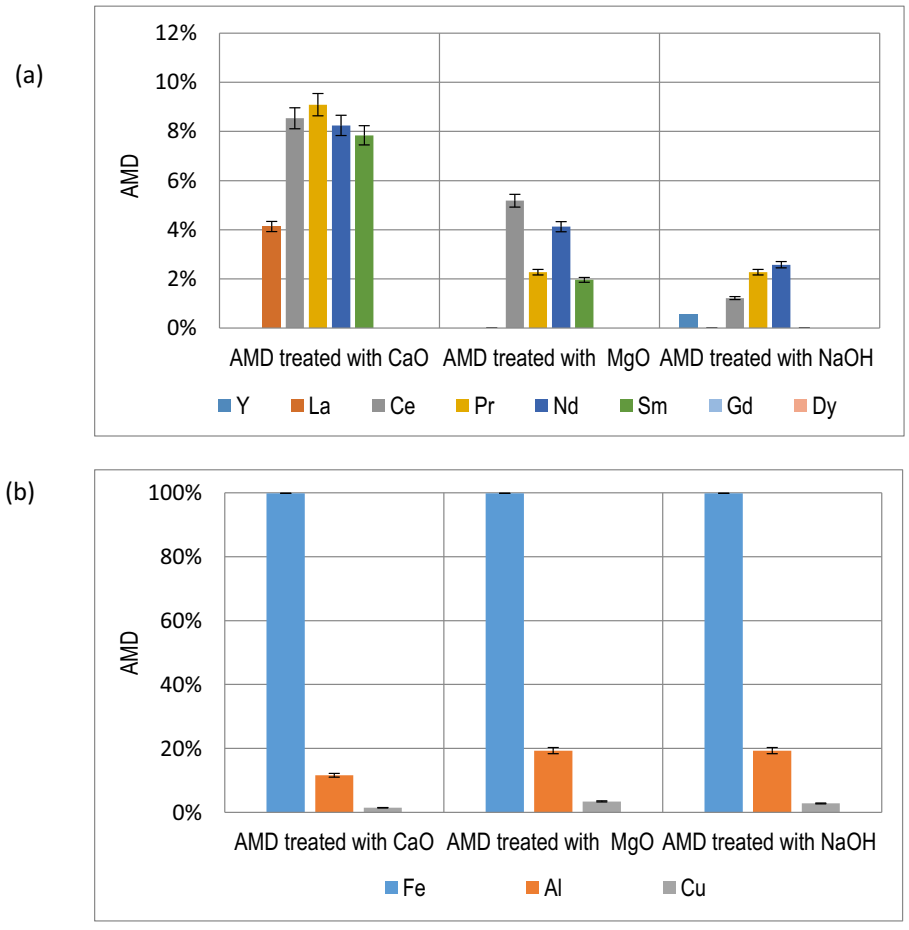

Fig. 3. The percentage of removal of a) REE and b) Fe, Al and Cu from treated AMD Poderosa Mine water using CaO(s), MgO(s) and NaOH as alkaline reagent. In Fig. 3a, for REE, error bars indicate that the removal percentage was less than 1%.

Table 2
Concentration (mg/L) of transition elements and REEs after oxidation pre-treatment of acid mine drainage (AMD).

TE and REE/(mg/L)	AMD treated with CaO	AMD treated with NaOH	AMD treated with MgO	AMD
Co	1,4 ± 0.2	1,4 ± 0.2	1,5 ± 0.2	1,4 ± 0.2
Cd	0,4 ± 0.05	0,4 ± 0.05	0,5 ± 0.05	0,4 ± 0.05
Ni	0,3 ± 0.04	0,3 ± 0.04	0,3 ± 0.04	0,3 ± 0.04
Ca	582 ± 80	147 ± 20	273 ± 40	161 ± 23
Mg	195 ± 30	172 ± 25	1025 ± 145	181 ± 25
Cu	110 ± 15	108 ± 15	107 ± 15	111 ± 15
Zn	108 ± 15	103 ± 15	105 ± 15	101 ± 15
Al	331 ± 45	302 ± 40	302 ± 40	375 ± 50
Fe	2,3 ± 0.3	2,2 ± 0.3	2,8 ± 0.3	1535 ± 220
Y	1,81 ± 0.2	1,78 ± 0.2	1,83 ± 0.2	1,79 ± 0.2
La	1,16 ± 0.1	1,21 ± 0.2	1,27 ± 0.2	1,21 ± 0.2
Ce	3,00 ± 0.4	3,24 ± 0.4	3,11 ± 0.4	3,28 ± 0.4
Pr	0,40 ± 0.04	0,43 ± 0.04	0,43 ± 0.04	0,44 ± 0.04
Nd	1,78 ± 0.2	1,89 ± 0.2	1,86 ± 0.2	1,94 ± 0.3
Sm	0,47 ± 0.04	0,51 ± 0.04	0,50 ± 0.04	0,51 ± 0.04
Eu	0,07 ± 0.01	0,07 ± 0.01	0,07 ± 0.01	0,07 ± 0.01
Gd	0,54 ± 0.07	0,54 ± 0.07	0,55 ± 0.07	0,54 ± 0.07
Tb	0,08 ± 0.01	0,09 ± 0.01	0,08 ± 0.01	0,09 ± 0.01
Dy	0,41 ± 0.04	0,40 ± 0.04	0,40 ± 0.04	0,40 ± 0.04
Ho	0,07 ± 0.01	0,07 ± 0.01	0,07 ± 0.01	0,07 ± 0.01
Er	0,15 ± 0.02	0,15 ± 0.02	0,15 ± 0.02	0,15 ± 0.02
Tm	0,02 ± 0.002	0,02 ± 0.002	0,02 ± 0.002	0,02 ± 0.002
Yb	0,10 ± 0.02	0,10 ± 0.02	0,10 ± 0.02	0,10 ± 0.02
Lu	0,01 ± 0.002	0,01 ± 0.002	0,01 ± 0.002	0,01 ± 0.002
Hf	0,41 ± 0.04	0,33 ± 0.04	0,43 ± 0.04	0,37 ± 0.04

precipitate as basaluminite [$Al_4(SO_4)(OH)_{10}{\cdot}5H_2O$] and REE will co-precipitate. This had been found by other when treating AMD with calcite ($CaCO_3$) (Ayora et al., 2016).

4.2. Concentration of REE from TAMD by using a sulfonic ion-exchange resin

The breakthrough curves, representing the variation of the C/C_0 ratio as a function of the treated effluent, as bed volumes (BV), are shown in Fig. 4. For simplicity, REE (a) and TE (b) breakthrough curves are shown separately. Fig. 4, shows also change in the pH during the sorption process. Initially the resin in sodium form is providing pH values above 5, to reach a value of 2 approaching the inlet feed pH. Even at these low pH values the sulfonic groups are having strong capacity to adsorb the REE elements. At the end of the experiment at 140 BV, the resin still shows extraction capacity for REE as C/C_0 is lower than 0.6 for most of the REE. The extraction decreases with the ionic radius, La been more favourably extracted than Lu, and Y being similar to Dy.

For a sulfonic functional group containing IX resin the extraction of REE occurs at pH more acidic than TE as it is more favoured for REE than for TE. The main metal extraction reaction involving a sulfonic group (R-SO_3H) and taking that the acidity constant of the sulfonic group ($\log K_a = 0.6$) means that it will be present typically as ionized form as described by Eq. (3):

$$R-SO_3H_r = R-SO_{3,r}^- + H^+ \; K_{a(r)} \quad (3)$$

where the general metal (M) extraction reaction is described by Eq. (4):

$$M(SO_4)_m^{(n-2m)+} + nR-SO_3H_r = (R-SO_3)_nM_r + nH^+ + mSO_4^{-2} \; K_{M/H} \quad (4)$$

and $R-SO_3H_r$ represents the sulfonic acid group on the IX resin.

Considering the acidity of the sulfonic group ($pK_a = -0.6$) the extraction is independent of the acidity range evaluated of the TAMD and extraction percentage only depends on the affinity of the sulfonic group for the metal ions, higher for trivalent ions REE, than for divalent ions (TE) as it is shown by the evolution of the breakthrough curves. For the case of divalent metal ions (TE) extraction is only takes place if the column pH is above 2, thus, opening the possibility to enhance the separation of divalent TE from REE. Al is extracted similarly to TE so the only means to separate is through selective precipitation with phosphate at fixed pH.

As Fig. 4 shows, REEs breakthrough reaches values of C/C_0 of 0.1 after 150 BV. However, a Yb, Dy and Y breakthrough reached extraction values 0.1 around 40 BV and saturation has not yet been reached ($C/C_0 = 1$) at the maximum volume treated (140 BV). For simplicity, column experiments were not extended to reach saturation to reproduce full-scale operation. Contrary for TE, the breakthrough occurs from 10 BV, with typical S shape curves and saturation is reached after 35 BV with the exception of Ca (II). Analysing the REE breakthrough profiles it is seen that LREE are more efficiently retained that HREE. Thus, for 140 BV, the highest C/C_0 values were measured 0.5 for Yb, 0.37 for Dy and Y,below 0.27 for Gd, Sm, and Nd, and below 0.1 for Pr, Ce and La. This sequence of C/C_0 shows the affinity of sulfonic resins on the separation of REE.

Elution of the loaded resin was carried out using 20 g/L sulfuric solutions. The elution curves for REE and TE (shown separately) are shown on Fig. 5. Elution of REEs and TEs occurs between 0.5 and 2 BV. For the case of REE, Ce, Y, La and Nd showed the longer tails, as expected from their higher concentration in the initial solution and the higher extraction factors. Taking into account the ratio of the BV values for breakthrough and the elution curves, a concentration factor of 5 were achieved for TE and higher than 20 could be achieved for most of the REE.

Similar sorption and desorption runs where carried out using also 0.5 M HCl as eluent solution, which is widely used in some hydrometallurgical applications. Two different types of concentrates of REE were generated, those where the total amount of REE ($\Sigma[REE]_{tot}$) was of 0.13 gREE/L and those with 0.24 gREE/L, just through adjusting the concentration of the leaching solution with either H_2SO_4 or HCl, respectively. These REE concentrates were used for the recovery of REE as REE-PO_4(s). The concentration of REE and TE in the concentrates generated is listed in Table 2 where the main TE interferences are associated to the presence of Al and Ca, Mg, Zn and Cu. Their presence is due to the observed extraction at the first 10BV of the breakthrough curves (Fig. 4b).

4.3. Recovery of REE by selective precipitation by phosphate from Poderosa mine AMD

The sulfuric and hydrochloric solutions from the IX regeneration stage containing a total REE concentration of 0.13 g REE/L. The concentrates were treated with a SQ excess of phosphate (of 2.5 or 40) at pH > 2.3, where the formation of REE-PO_4(s) starts (see Fig. 2) and using NaOH as

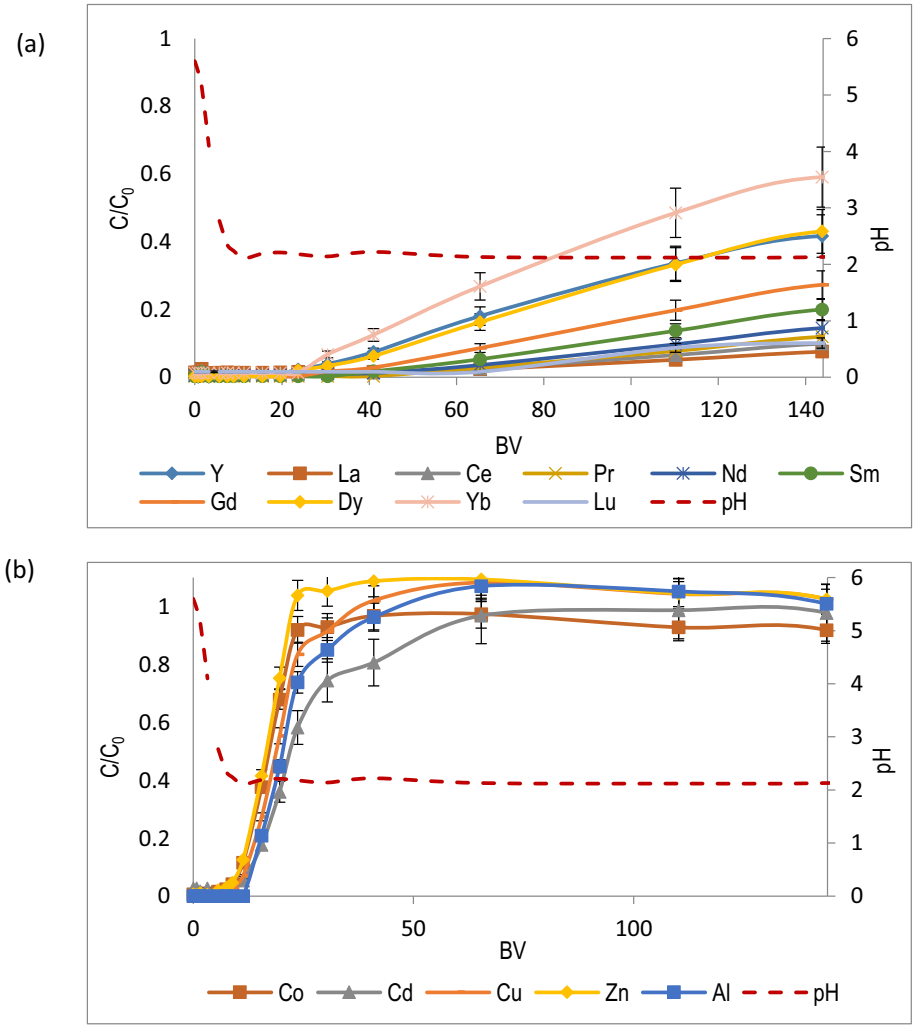

Fig. 4. Extracted fraction of REE (a) and transition metals (b) from treated AMD as a function of treated bed volumes of effluent (BV) with ion-exchange resin. Initial TAMD was acidified to pH 2 to increase the selectivity factors for REE extraction.

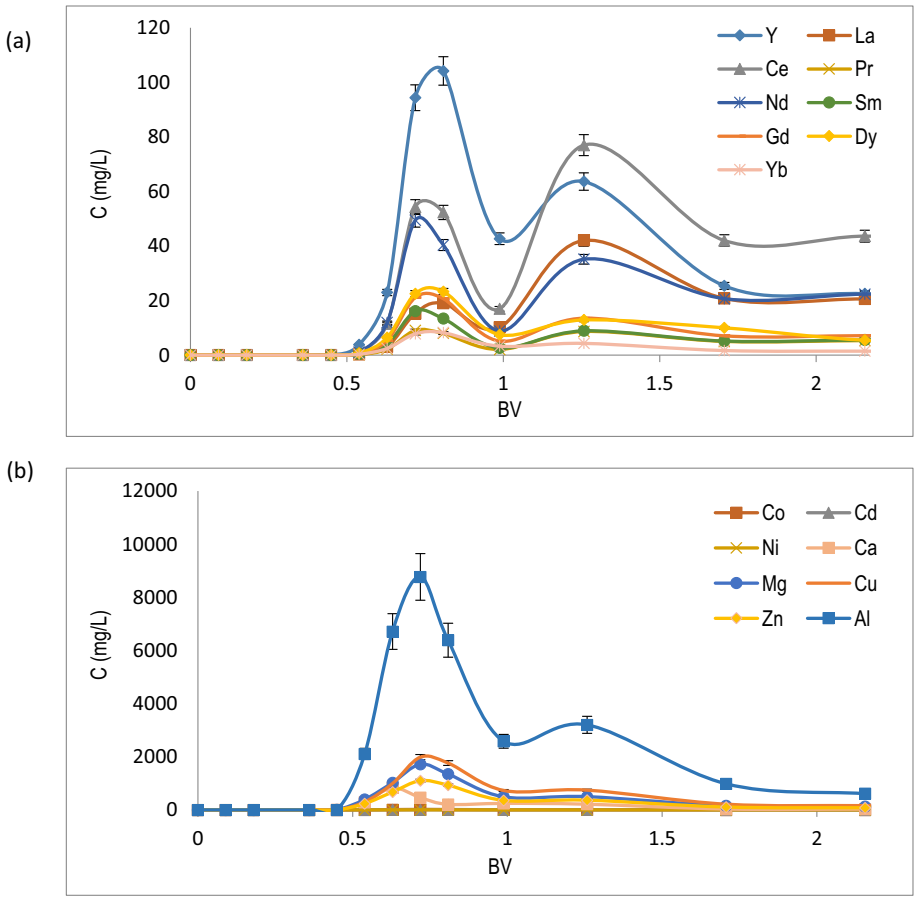

Fig. 5. Regeneration curves C(mg/L) of the SPC11706 resin for a) REE and b) TM as a function of the BV of the leaching solution.

neutralization reagent. In a pH range of 2.3 to 2.5, recovery ratios (%) of REE were below 20% (data not shown) while recovery ratios of TE where below 5% for both sulfuric and hydrochloric solutions.

The increase of pH and the SQ excess up to a ratio of 40 favour the formation of REE-phosphates.

Recovery percentages of REE from concentrates generated in the concentration stage with IX, with a total REE concentration of 0.24 g REE/L as a function of the Fe(III) pre-treatment stage (e.g., NaOH, CaO(s), and MgO(s)) are summarized in Fig. 6.

The higher REE recovery achieved was for phosphate doses with SQ ratios of 40 with recovery ratios higher than 85%, with the exception of Y with values from 60 to 80%. The increase of phosphate concentration increased the recovery ratio of REE, whereas the recovery ratios of TE were below 20%. Finally, it is worth to mention that efficient REE precipitation ratios are obtained in samples pre-treated with MgO(s) and CaO(s) not requesting for potentially higher doses of phosphate when compared with samples pre-treated with NaOH for Fe(III) removal. This leads to postulate that phosphate precipitation works independently of the type of neutralization used for Fe removal.

Sampled solids showed in general an amorphous form according to XRD results, as it is shown in Fig. 7a for NaOH as example. Spectrum for samples neutralize using CaO and MgO not shown.

Kim and Osseo-Asare (2012) found that for La and Ce, the stability region of the $REEPO_4$(s) is different, depending on differences in the crystallinity and aging stages. The stability region of the $REEPO_4$ is smaller for the less crystalline phosphates, suggesting that amorphization may be an effective method for enhancing the dissolution of monazite. Then, this lower crystallinity was identified as beneficial for the subsequent processing stages of the REE-phosphates generated.

Samples collected from the phosphate precipitation trials were subjected to a heat treatment at 1050 °C for 4 h for its crystallization, the results are shown in Fig. 7b. As it is shown Fig. 7b, XRD results for a rich REE containing concentrate (REE_{tot} > 0.24 mgREE/L) pre-treated for Fe(III) removal with NaOH for a phosphate SQ ratio of 40, the major mineral phases were Praseodymium Phosphate ($PrPO_4$) and Cheralite ($CePO_4$) in which the Ce could be replaced by other elements as La, Xenotime (YPO_4) is also notably present in the precipitate. It could not be discarded that the $PrPO_4$(s) could be a mixture of other REE as Sm and Nd. Finally, the other minor phase identified was aluminium phosphate ($AlPO_4$) and calcium magnesium yttrium phosphate ($Ca,MgYPO_4$) was also identified.

The samples pre-treated for Fe(III) removal with CaO(s) and MgO(s), showed similar results to those obtained with NaOH pre-treatment for Fe(III) removal. The major phases were Praseodymiun Phosphate ($PrPO_4$) and Cheralite ($CePO_4$), Xenotime (YPO_4) and Aluminium Phosphate ($AlPO_4$).

Although Kim and Osseo-Asare (2012) concluded that the introduction of sulfate ions diminishes the stability domains of the solid metal phosphates, replacing them with solid metal sulfates and or soluble metal sulfate complexes, in this study the presence of REE-sulfates or mixed REE-phosphate-sulfate mineral phases were not detected.

Results obtained could be used to define the chemical basis for the selective recovery by precipitation with phosphates and for commercial process of monazite digestion in sulfuric acid (Jha et al., 2016; Xie et al., 2014).

Fig. 8, describes the integration process of the pre-treatment stage for Fe removal, concentration stage with IX and precipitation stage with phosphate solutions.

At industrial scale the Fe removal stage would be completed using NaOH to reduce the presence of Ca(II) and Mg(II) while the total oxidation of Fe(II) to Fe(III) will be carried out by using H_2O_2. Finally, the potential integration of a concentration stage of the REE by using a sulfonic IX resin as Purolite SPC11706 and recovery of the acid sulfuric excess by using acid resistance nanofiltration membranes as Duracid or

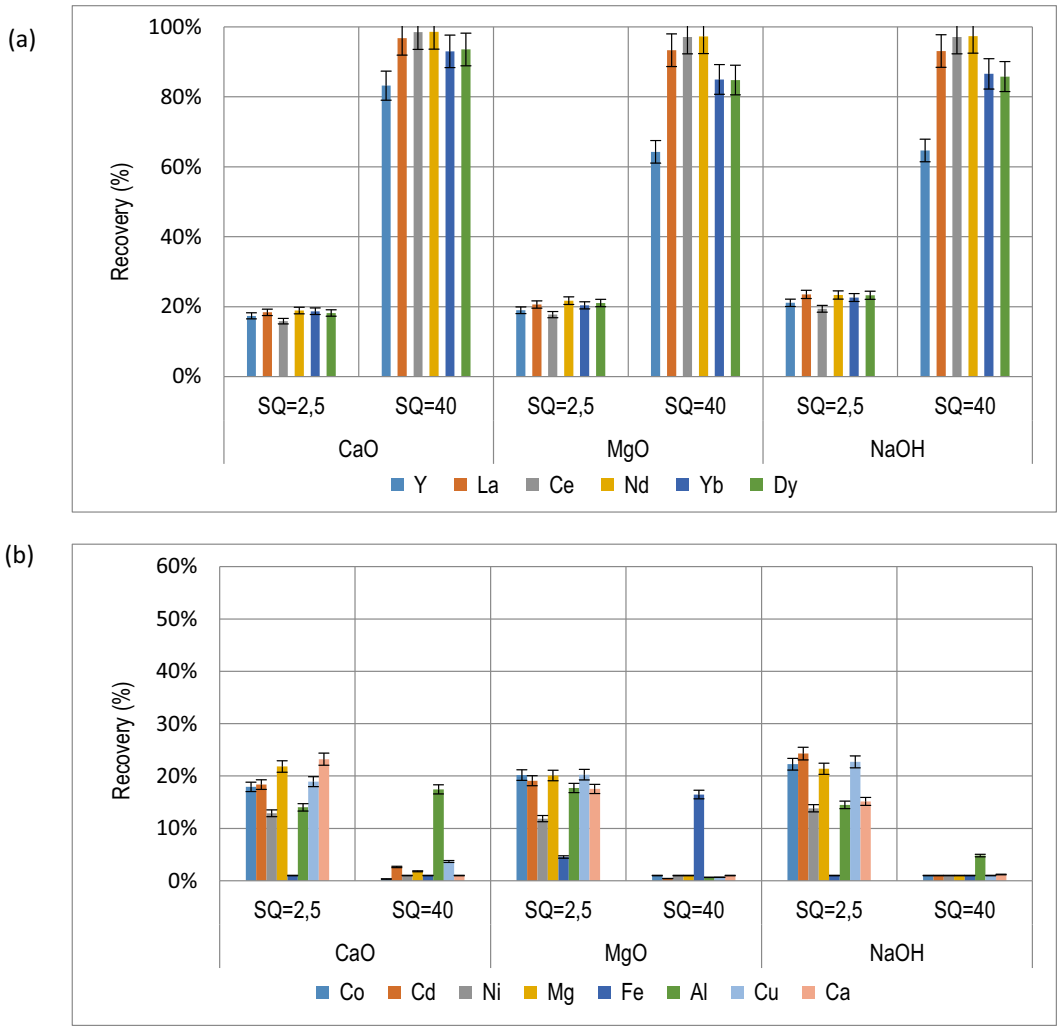

Fig. 6. Recovery ratios (%) of REE (a) and TE (b) for eluates with >240 mg REE/L at pH 2.5 as a function of phosphate stoichiometric excess (SQ 2,5 and 40). Rich REE-containing eluates REE > 240 mg/L where generated from AMD pre-treated for Fe(III) removal with CaO(s), MgO(s) and NaOH.

Hydracore 40pHT. As it has been demonstrated by López et al. (2019a) this will provide a rich concentrate of REE up to 0.6–0.8 gREE/L, and the recovery of H_2SO_4 to be reused on the IX regeneration stage. Then, many options associated to by-products recovery, in the new scenario, could be linked with the need of the mining industry to search economically and sustainable options to reuse mine waters. The treated water can then be discharged into natural water bodies. During the treatment train the valuable components typically disposed as waste are being investigated, to promote their recovery.

Recently, Royer-Lavallée et al. (2020) critically reviewed the recovery of REEs from AMD and concluded that could be an alternative to their conventional mining, given that REE are relatively highly concentrated in AMD. From the pre-concentration options evaluated through passive and active treatment, the second option including additional stages of pre-concentration with ion-exchange resins are promising from an economic, environmental and sustainability point of view. The use of combination of sorption and precipitation as main processes for REE removal from AMD are more relevant options. Even limited research projects, as it is the case of this work, proposes the selective precipitation as a technological option for the REE removal from AMD, but its high removal ratios justifies further research. Pilot -scale experiments for REE recovery from AMD remediation have already been conducted and this emerging option has shown economic liability. Further research is needed to demonstrate the performance of evaluated schemes at full scale (Stewart et al., 2017; Ziemkiewicz et al., 2018).

5. Conclusions

The pre-treatment stage of Fe removal by pre-oxidation with H_2O_2 was successfully achieved and the solution could be treated increasing the pH with removal efficiencies of Fe higher than 99.9% and low removal ratios of REE (values below 5%). The three alkaline reagents used, CaO(s), MgO (s) and NaOH result in a similar high efficiency for Fe removal but NaOH gave the lowest REE removal rates below 2%, significantly lower than those of CaO(s) and MgO(s).

REE recovery from the leachates can be achieved by means of precipitation with phosphates. The percentage of $REEPO_4$ (s) precipitation is enhanced at pH 2.3 to 2.5 and molar phosphate stoichiometric ratios increasing from 2.5 to 40. Under such conditions, H_2SO_4 provided the better performance and the nature of alkaline agent used in the Fe removal (CaO, MgO or NaOH) did not have any relevant influence on this stage.

XRD analysis of the precipitates collected indicated the formation of non-crystalline mineral phases, which after thermal treatment at 1050 °C transform into crystalline Preseodymium Phosphate ($PrPO_4$) and Cheralite ($(Ce,La)PO_4$) and Xenotime (YPO_4) as major phases.

These results are used to define the chemical basis for a selective recovery of REE from AMD by a concentration using a sulfonic ion-exchange resin and further precipitation with phosphates. This process could also be useful for REE extraction after monazite digestion in sulfuric acid.

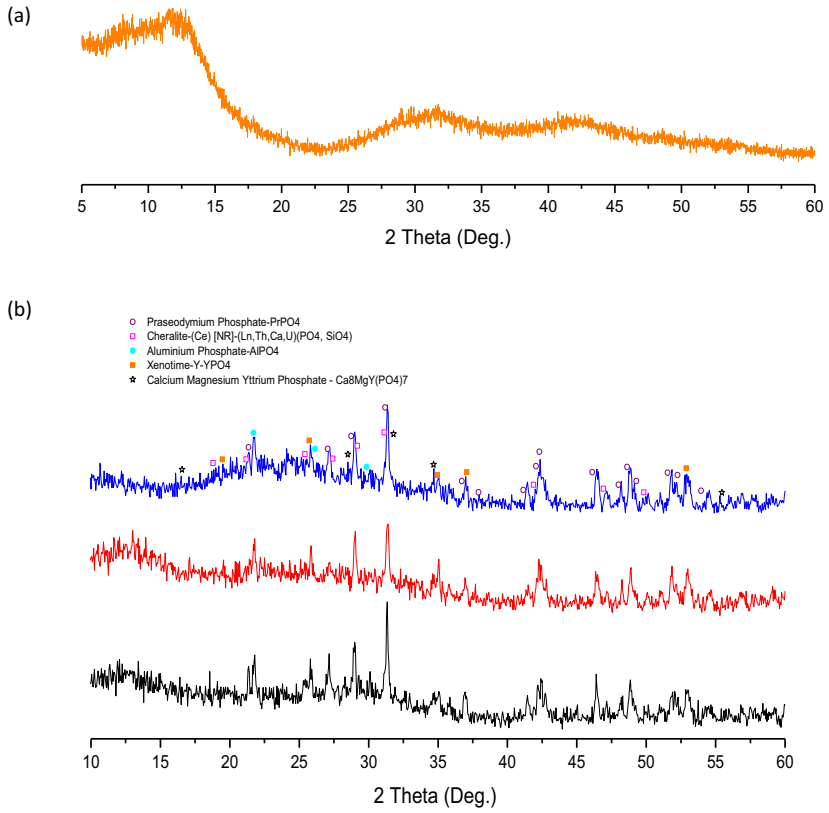

Fig. 7. (a) XRD result of the sample for a rich REE containing concentrate (REE_{tot} > 0.24 gREE/L) pre-treated for Fe(III) removal with NaOH for a phosphate SQ ratio of 40 without thermal treatment example. (b) XRD result for a rich REE containing concentrate (REE_{tot} > 0.24 mgREE/L) pre-treated for Fe(III) removal with NaOH (black line spectrum), Fe(III) removal with CaO(s) (red line spectrum) and Fe(III) removal with MgO(s) (blue line spectrum) for a phosphate SQ ratio of 40 after thermal pre-treatment at 1050 °C over 4 h.

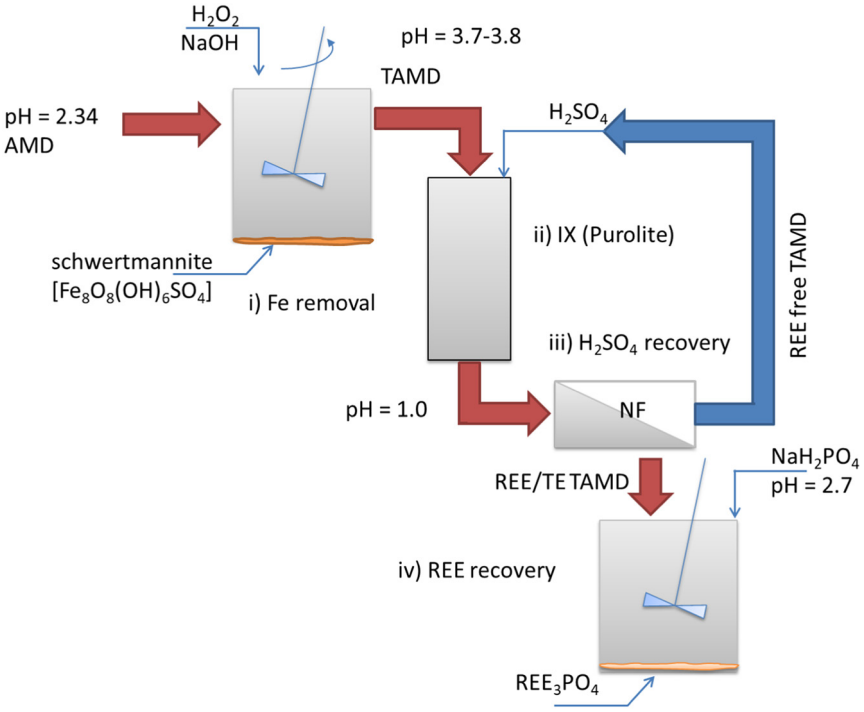

Fig. 8. Proposed treatment of an AMD including i) total oxidation of Fe(II) to Fe(III) and precipitation with NaOH ii) concentration of valuable metals with a sulfonic IX resin (Purolite SPC11706); iii) recovery of H_2SO_4 excess and concentration of valuable metals with membrane acidic resistant nanofiltration and; iv) selective precipitation of REE as phosphates.

CRediT authorship contribution statement

M. Hermassi: Conceptualization, Data curation, Formal analysis, Writing - original draft, analysis. **M. Granados**: Conceptualization, Funding acquisition, Writing - review & editing. **C. Valderrama**: Conceptualization, Funding acquisition, Writing - review & editing. **C. Ayora**: Conceptualization, Funding acquisition, Writing - review & editing. and **J. L. Cortina**: Conceptualization, Funding acquisition, Resources, Supervision, Writing - review & editing.

Declaration of competing interest

The authors declare that they have no known competing financial interests or personal relationships that could have appeared to influence the work reported in this paper.

Acknowledgements

This research was supported by the W4V project (ref. PID2020-114401RB-C21) and the R2MIT project (CTM2017-85346-R) financed by the Ministerio de Economía y Competitividad (MINECO), the Catalan Government (Project Ref. 2017SGR312), Spain. And the European Commission through the OpenInnotrain project MSCA-RISE-2018-823971. Additionally, the Kempe Foundation is thanked for their financial support to Dr. Mehrez Hermassi at Umeå University (projekt med referensnummer SMK-1856). We also want to thank the contribution of Purolite Spain (J. Barios / R. Salvatierra) for the supply of IX Resins, to G. Chavez for their help during the experimental work and to the Institut de Diagnosi Ambiental i Estudis de l'Aigüa -IDAEA, Consejo Superior de Investigaciones Científicas-CSIC for the ICP analysis.

References

Ackman, T.E., 1982. Sludge disposal from acid mine drainage treatment. Report of Investigation 8672. US Bureau of Mines, Pittsburgh.
Akcil, A., Koldas, S., 2006. Acid mine drainage (AMD): causes, treatment and case studies. J. Clean. Prod. 14, 1139–1145.
Al-Zoubi, H., Rieger, A., Steinberger, P., Pelz, W., Haseneder, R., Härtel, G., 2010. Optimization study for treatment of acid mine drainage using membrane technology. Sep. Sci. Technol. 45, 2004–2016.
Ayora, C., Caraballo, M.A., Macias, F., Rötting, T.S., Carrera, J., Nieto, J.M., 2013. Acid mine drainage in the iberian Pyrite Belt: 2. Lessons learned from recent passive remediation experiences. Environ. Sci. Pollut. Res. 20, 7837–7853.
Ayora, C., Macías, F., Torres, E., Nieto, J.M., 2015. Rare earth elements in acid mine drainage. XXXV Reun. La Soc. Española Mineral, pp. 1–22.
Ayora, C., Macías, F., Torres, E., Lozano, A., Carrero, S., Nieto, J.M., Pérez-López, R., Fernández-Martínez, A., Castillo-Michel, H., 2016. Recovery of rare earth elements and yttrium from passive-remediation systems of acid mine drainage. Environ. Sci. Technol. 50, 8255–8262.
Binnemans, K., Jones, P.T., Blanpain, B., Van Gerven, T., Yang, Y., Walton, A., Buchert, M., 2013. Recycling of rare earths: a critical review. J. Clean. Prod. 51, 1–22.
Blanc, P., Lassin, A., Piantone, P., Azaroual, M., Jacquemet, N., Fabbri, A., Gaucher, E.C., 2012. Thermoddem: a geochemical database focused on low temperature water/rock interactions and waste materials. Appl. Geochem. 27, 2107–2116.
Evangelou, V.P., Zhang, Y.L., 1995. Critical reviews in environmental science and technology a review: pyrite oxidation mechanisms and acid mine drainage prevention a review: pyrite oxidation mechanisms and acid mine drainage prevention. Crit. Rev. Environ. Sci. Technol. 25, 141–199.
Gupta, N.K.C.K., 2005. Extractive Metallurgy of Rare Earths.
Habashi, F., 2013. Extractive metallurgy of rare earths. Can. Metall. Q. 52, 224–233.
Hedin, R.S., Watzlaf, G.R., Nairn, R.W., 1994. Passive treatment of acid mine drainage with limestone. J. Environ. Qual. 23, 1338–1345.
Hermassi, M., Granados, M., Valderrama, C., Ayora, C., Cortina, J.L., 2021. Recovery of rare earth elements from acidic mine waters by integration of a selective chelating ion- exchanger and a solvent impregnated resin. J. Environ. Chem. Eng. 9, 105906.
Iftekhar, S., Srivastava, V., Sillanpää, M., 2017. Enrichment of lanthanides in aqueous system by cellulose based silica nanocomposite. Chem. Eng. J. 320, 151–159.
Jha, M.K., Kumari, A., Panda, R., Rajesh Kumar, J., Yoo, K., Lee, J.Y., 2016. Review on hydrometallurgical recovery of rare earth metals. Hydrometallurgy 165, 2–26.
Jorjani, E., Shahbazi, M., 2016. The production of rare earth elements group via tributyl phosphate extraction and precipitation stripping using oxalic acid. Arab. J. Chem. 9, S1532–S1539.
Khawassek, Y.M., Eliwa, A.A., Gawad, E.A., Abdo, S.M., 2015. Recovery of rare earth elements from El-sela effluent solutions. J. Radiat. Res. Appl. Sci. 8, 583–589.
Kim, E., Osseo-Asare, K., 2012. Aqueous stability of thorium and rare earth metals in monazite hydrometallurgy: eh-pH diagrams for the systems th-, ce-, La-, nd- (PO4)-(SO4)-H2O at 25 °C. Hydrometallurgy 113–114, 67–78.
Kulczycka, J., Kowalski, Z., Smol, M., Wirth, H., 2016. Evaluation of the recovery of rare earth elements (REE) from phosphogypsum waste - case study of the WIZÓW chemical plant (Poland). J. Clean. Prod. 113, 345–354.
López, J., Reig, M., Gibert, O., Torres, E., Ayora, C., Cortina, J.L., 2018. Application of nanofiltration for acidic waters containing rare earth elements: influence of transition elements, acidity and membrane stability. Desalination 430, 33–44.
López, J., Reig, M., Yaroshchuk, A., Licon, E., Gibert, O., Cortina, J.L., 2018. Experimental and theoretical study of nanofiltration of weak electrolytes: SO42−/HSO4−/H+ system. J. Membr. Sci. 550, 389–398.
López, J., Reig, M., Gibert, O., Cortina, J.L., 2019. Integration of nanofiltration membranes in recovery options of rare earth elements from acidic mine waters. J. Clean. Prod. 210, 1249–1260.
López, J., Reig, M., Gibert, O., Cortina, J.L., 2019. Recovery of sulphuric acid and added value metals (Zn, cu and rare earths) from acidic mine waters using nanofiltration membranes. Sep. Purif. Technol. 212, 180–190.
Machacek, E., Richter, J.L., Habib, K., Klossek, P., 2015. Recycling of rare earths from fluorescent lamps: value analysis of closing-the-loop under demand and supply uncertainties. Resour. Conserv. Recycl. 104, 76–93.
Martí-Calatayud, M.C., Buzzi, D.C., García-Gabaldón, M., Ortega, E., Bernardes, A.M., Tenório, J.A.S., Pérez-Herranz, V., 2014. Sulfuric acid recovery from acid mine drainage by means of electrodialysis. Desalination 343, 120–127.
Meschke, K., Hansen, N., Hofmann, R., Haseneder, R., Repke, J.U., 2018. Characterization and performance evaluation of polymeric nanofiltration membranes for the separation of strategic elements from aqueous solutions. J. Memb. Sci. 546, 246–257.
Mullett, M., Fornarelli, R., Ralph, D., 2014. Nanofiltration of mine water: impact of feed pH and membrane charge on resource recovery and water discharge. Membranes (Basel) 4, 163–180.
Nleya, Y., Simate, G.S., Ndlovu, S., 2016. Sustainability assessment of the recovery and utilisation of acid from acid mine drainage. J. Clean. Prod. 113, 17–27.
Olías, M., Cánovas, C.R., Basallote, M.D., Lozano, A., 2018. Geochemical behaviour of rare earth elements (REE) along a river reach receiving inputs of acid mine drainage. Chem. Geol. 493, 468–477.
Parkhurst, D.L., Appelo, C.A.J., 1999. User's guide to PHREEQC (Version 2): a computer program for speciation, batch-reaction, one-dimensional transport, and inverse geochemical calculations. U.S. Geol. Surv. 312.
Pramanik, B.K., Shu, L., Jegatheesan, J., Shah, K., Haque, N., Bhuiyan, M.A., 2019. Rejection of rare earth elements from a simulated acid mine drainage using forward osmosis: the role of membrane orientation, solution pH, and temperature variation. Process Saf. Environ. Prot. 126, 53–59.
Ramasamy, D.L., Porada, S., Sillanpää, M., 2019. Marine algae: a promising resource for the selective recovery of scandium and rare earth elements from aqueous systems. Chem. Eng. J. 371, 759–768.
Reig, M., Vecino, X., Hermassi, M., Valderrama, C., Gibert, O., Cortina, J.L., 2019. Integration of selectrodialysis and solvent-impregnated resins for Zn(II) and Cu(II) recovery from hydrometallurgy effluents containing As(V). Sep. Purif. Technol. 229, 115818.
Riley, E., Dutrizac, J.E., 2017. The behaviour of the rare earth elements during the precipitation of ferrihydrite from sulphate media. Hydrometallurgy 172, 69–78.
Royer-Lavallée, A., Neculita, C.M., Coudert, L., 2020. Removal and potential recovery of rare earth elements from mine water. J. Ind. Eng. Chem. 89, 47–57.
Samonov, A.E., 2011. New data on mineral forms of rare metals in phosphogypsum wastes. Dokl. Earth Sci. 440, 1312–1315.
Sánchez-España, J., Yusta, I., Diez-Ercilla, M., 2011. Schwertmannite and hydrobasaluminite: a re-evaluation of their solubility and control on the iron and aluminium concentration in acidic pit lakes. Appl. Geochem. 26, 1752–1774.
Simate, G.S., Ndlovu, S., 2014. Acid mine drainage: challenges and opportunities. J. Environ. Chem. Eng. 2, 1785–1803.
Stewart, B.B., Capo, R.C., Hedin, B.C., Hedin, R.S., 2017. Rare earth element resources in coal mine drainage and treatment precipitates in the Appalachian Basin, USA. Int. J. Coal Geol. 169, 28–39.
Vaziri Hassas, B., Rezaee, M., Pisupati, S.V., 2020. Precipitation of rare earth elements from acid mine drainage by CO2 mineralization process. Chem. Eng. J. 399, 125716.
Viadero, R.C., Wei, X., Buzby, K.M., 2006. Characterization and dewatering evaluation of acid mine drainage sludge from ammonia neutralization. Environ. Eng. Sci. 23, 734–743.
Wang, L., Huang, X., Yu, Y., Zhao, L., Wang, C., Feng, Z., Cui, D., Long, Z., 2017. Towards cleaner production of rare earth elements from bastnaesite in China. J. Clean. Prod. 165, 231–242.
Wu, S., Wang, L., Zhao, L., Zhang, P., El-Shall, H., Moudgil, B., Huang, X., Zhang, L., 2018. Recovery of rare earth elements from phosphate rock by hydrometallurgical processes – a critical review. Chem. Eng. J. 335, 774–800.
Xie, F., Zhang, T.A., Dreisinger, D., Doyle, F., 2014. A critical review on solvent extraction of rare earths from aqueous solutions. Miner. Eng. 56, 10–28.
Zhang, K., Kleit, A.N., Nieto, A., 2017. An economics strategy for criticality – application to rare earth element yttrium in new lighting technology and its sustainable availability. Renew. Sust. Energ. Rev. 77, 899–915.
Zhong, C.M., Xu, Z.L., Fang, X.H., Cheng, L., 2007. Treatment of acid mine drainage (AMD) by ultra-low-pressure reverse osmosis and nanofiltration. Environ. Eng. Sci. 24, 1297–1306.
Ziemkiewicz, P., Vass, C., Liu, X., Ren, P., Noble, A., 2018. Design and evaluation of an acid leaching solvent extraction process to extract rare earth elements from acid mine drainage precipitates. 2018 Annual USDOE/NETL Pittsburg, USA.